Progress In Electromagnetics Research C, Vol. 101, 95–104, 2020

Compact Dual Polarised Branch-Line Printed Inverted-F Antenna Covering Both Cellular and Non-Cellular Bands with Independent Tuning

Anupa Chatterjee[1, *], Manas Midya[1], Laxmi P. Mishra[2], and Monojit Mitra[1]

Abstract—In this paper a novel branch-line printed inverted-F antenna (IFA) loaded with a rectangular complementary split-ring resonator (CSRR) is proposed, designed, and experimentally studied. The proposed antenna shows four operating frequencies and can be used for various cellular and wireless applications (900 MHz/3.5 GHz/4.2 GHz/5.5 GHz). The antenna is compact in size having dimensions $0.059\lambda_0 \times 0.053\lambda_0 \times 0.002\lambda_0$ at the lowest resonance frequency. Each of the bands is independently tunable and shows circular polarisation (CP) in the WLAN band with linear polarization (LP) in the other three bands. The axial ratio (AR) bandwidth is 1.82% in WLAN band. The simulated and fabricated results are reported in terms of S-parameters and radiation pattern. The prototype of the antenna has been fabricated and measured using VNA and simulation done in ANSYS HFSS.

1. INTRODUCTION

The recent surge of wireless communication systems has increased the use of modern wireless devices over the last decades. System applications such as WLAN and Wi-MAX have frequency bands which are far from the cellular bands (GSM/DCS). So to design an antenna which can cover both cellular and non-cellular bands together is proved to be a difficult task for researchers. Multiple services at different frequencies while limiting the overall size of the wireless devices are a major challenge for today's researcher. Thus a single antenna offering multiband operation is the best alternative. In literature, planar monopole antennas are found to be a good candidate for multiband operation due to their low profile, light weight, and easy fabrication. In [1], a folded slit technique has been proposed, but it covers a small bandwidth only GSM/DCS/PCS/UMTS bands. In [2], the monopole antenna is a bended T-shaped structure with a parasitic shorted element. However, its large ground plane makes its application limited. A planar monopole antenna with an E-shaped slot on the ground plane for triple frequency bands is proposed in [3], but the size of the antenna is large. Recently, a multiband antenna with three radiating strips is proposed in [4], but since it is fabricated on a single side of the substrate, the system ground plane becomes big. In [5], a printed multiband antenna with a rectangular patch and truncated ground plane is proposed. However, again the total size of the antenna is large. In [6, 7], triple band monopole antennas with multi-stub loading and pairs of SRRs are designed respectively, but they use costly substrate, and the size becomes the constraint. The shortcomings of the above antennas are overcome by inverted-F antennas. In the early twentieth century, the theory behind printed IFA was first introduced. One of the main advantages of IFA is that by just tuning the dimensions of IFA, impedances can be well matched without the need of any external circuitry. Again there are advantages in terms of dimensions, since a quarter wavelength patch is shorted at one end, and current at the end

Received 4 March 2020, Accepted 9 April 2020, Scheduled 17 April 2020
* Corresponding author: Anupa Chatterjee (anupa.c12@gmail.com).
[1] Department of Electronics & Telecommunication Engineering, Indian Institute of Engineering Science & Technology, Shibpur, India. [2] Department of Electronics and Communication Engineering, Siksha o Anusandhan (Deemed to be University), Bhubaneswar, Odisha 751030, India.

of the patch is no longer needed to be zero, thus it acquires the features of a half wavelength patch. A dual-band printed IFA is studied in [8]. Later improved IFAs with multiband features are proposed in [9–11]. In [12], a multiband IFA is designed with a multi branching technique, but again its complex structure makes its application limited. Though all the antennas give multiband characteristics, either the height of the antennas from the ground plane is too large, the ground plane itself is too big, the bands covered are limited, or the operating frequency is not tunable. Again on the other hand, CP is preferred in WLAN because it can minimize multipath effect and is insensitive to transmitter-receiver orientation. Dual polarised dual band and dual polarised multiband monopole antennas are studied in [13–17], respectively. In [18], a compact CPW-fed circular polarised antenna for WLAN is studied. The main drawback of printed antennas is their narrow frequency bandwidth which is overcome by Log-periodic dipole arrays (LPDA) as discussed in [19]. Although its gain is high, the large size limits its application in small form factor devices. In this paper, a novel branch line printed IFA with a microstrip line feed and loaded with rectangular CSRR is designed.

The proposed antenna has a dimension of $20 \times 18\,\text{mm}^2$ and can be used for quad band application in 900 MHz/3.5 GHz/4.2 GHz/5.5 GHz with independent control of each frequency band. It shows optimum CP characteristics in WLAN band.

2. ANTENNA DESIGN AND ANALYSIS

In this section, antenna design and analysis are discussed. This section is divided into two subsections; 2.1, Antenna design; 2.2, Independent frequency tuning operations.

2.1. Antenna Design

The proposed quad band printed IFA with two branch strips sharing a common feed with a common short is printed on a low cost FR4 substrate having dielectric constant, $\varepsilon_r = 4.4$, loss tangent $\delta = 0.02$, and thickness $h = 0.8\,\text{mm}$ as shown in Figure 1(a). The structure is then loaded with CSRR on the small sized ground plane as shown in Figure 1(b). It utilizes two different resonant paths. The longer one controls the resonance around 900 MHz and 5.5 GHz while the shorter one controls the resonance around 3.5 GHz. The position of CSRR is offset to introduce an additional band at 4.2 GHz, thus generating the quad band behavior. Photographs of the fabricated prototype are shown in Figure 1(c).

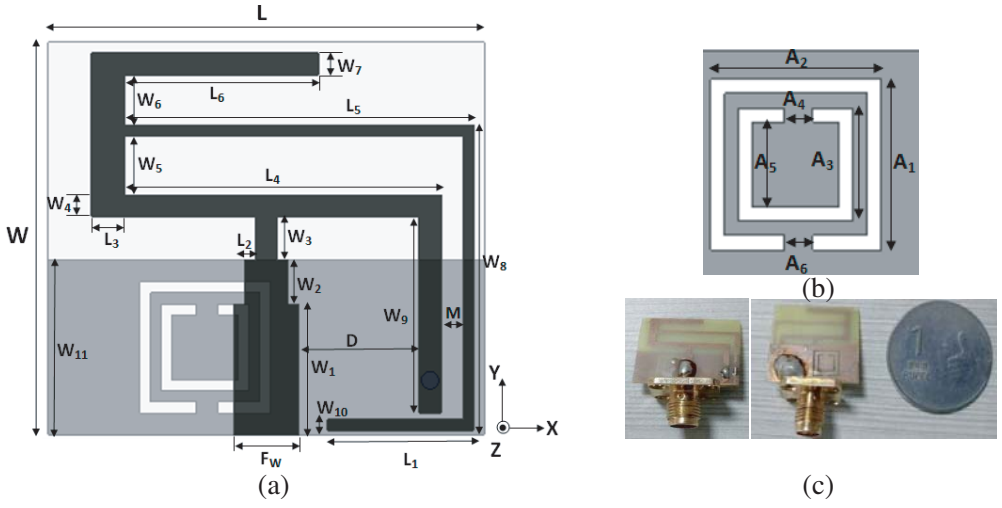

Figure 1. Proposed antenna geometry and photograph; (a) Schematic diagram with $L = 20$, $W = 18$, $F_w = 3$, $L_1 = 6.5$, $L_2 = 1$, $L_3 = 1.5$, $L_4 = 14.5$, $L_5 = 16$, $L_6 = 8.9$, $W_1 = 6$, $W_2 = 2$, $W_3 = 2$, $W_4 = 1$, $W_5 = 2.7$, $W_6 = 2.3$, $W_7 = 1$, $W_8 = 14$, $W_9 = 9$, $W_{10} = 0.5$, $W_{11} = 8$, $D = 5.5$, $M = 1$ (all dimensions are in mm). (b) The CSRR with $A_1 = A_2 = 6$, $A_3 = 4$, $A_5 = 3$, $A_4 = A_6 = 1$ (all dimensions are in mm). (c) Photograph of the prototype.

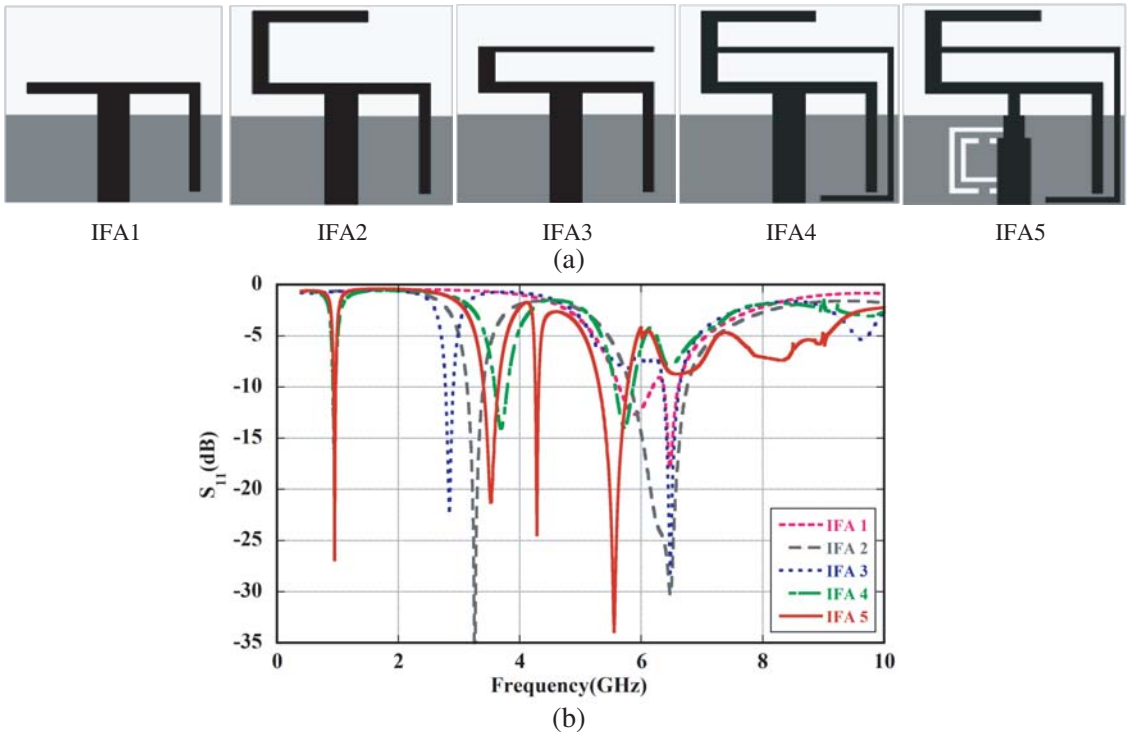

Figure 2. (a) Steps of improvement. (b) Reflection Coefficient (S_{11}) of antenna for the five implementation steps.

Figures 2(a) and 2(b) show the evolution of the proposed antenna structure and the reflection coefficient variation with frequency for five different design steps.

The design of the proposed antenna is influenced from a T-shaped monopole antenna, and taking symmetric arms gives a single band of resonance, but asymmetric arms give rise to dual bands, which are calculated from the basic design equation given below:

$$\lambda_g = \frac{\lambda_0}{\sqrt{\varepsilon_{\text{eff}}}} \tag{1}$$

where λ_g is the guided wavelength, λ_0 the free space wavelength, and ε_{eff} the effective permittivity of the substrate. For miniaturization, the longer arm of the asymmetric T-shaped monopole is shorted to the ground plane by a shorting pin to give rise to the IFA 1 structure, Figure 2(a), with dual bands at 5.8 GHz and 6.4 GHz. In the next step, IFA2, the left arm is extended upward which further shifts the lower frequency. The total length of the arm responsible for this new resonance is:

$$L_{\text{IFA2}} = (L_3 + L_4)/2 + W_5 + W_6 + W_7 + L_6 = 22.9\,\text{mm} \tag{2}$$

Now at resonance, the length L_{IFA2} is approximately equal to one quarter-wavelength of the center operating frequency in free space $\lambda_c/4$ [20].

$$f_{\text{IFA2(lower)}} = \frac{C}{4L_{\text{IFA2}}} = 3.275\,\text{GHz} \tag{3}$$

From the simulation results, the lower resonance is at 3.26 GHz. For IFA 3 structure, the simulated resonance is at 2.84 GHz. The total length of the arm responsible for the resonance is:

$$L_{\text{IFA3}} = (L_3 + L_4)/2 + W_5 + L_5 = 26.7\,\text{mm} \tag{4}$$

Therefore,

$$f_{\text{IFA3(lower)}} = \frac{C}{4L_{\text{IFA3}}} = 2.808\,\text{GHz} \tag{5}$$

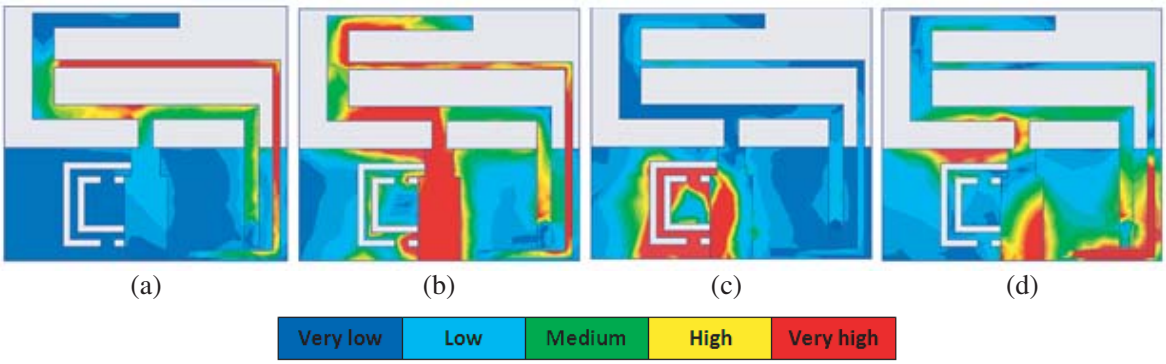

Figure 3. Surface current distributions (A/m) on the structures at (a) 900 MHz; (b) 3.5 GHz; (c) 4.2 GHz; (d) 5.5 GHz.

The IFA4 structure combines both, but with the lower branch extended. This reduces the lowest resonant frequency and left shifts it. The total length of the arm responsible for the lowest resonant frequency is:

$$L_{\text{IFA4}} = (L_3 + L_4)/2 + W_5 + L_5 + W_8 + L_1 = 47.2\,\text{mm} \tag{6}$$

Thus,

$$f_{\text{IFA4(lowest)}} = \frac{C}{4L_{\text{IFA4}}} = 0.968\,\text{GHz} \tag{7}$$

The calculated result nearly matches the simulated results at 0.934 GHz. The other higher resonances are slightly affected due to mutual coupling. In IFA 5, the CSRR introduces the third band at 4.2 GHz. The proposed antenna thus produces a quad band at 900 MHz(GSM900)/3.5 GHz(5G)/4.2 GHz(C-band)/5.5 GHz(WLAN). The -10 dB impedance bandwidths are 86 MHz (878–964 MHz), 262 MHz (3393–3655 MHz), 97 MHz (4224–4321 MHz), 514 MHz (5300–5814 MHz), and the AR bandwidth at the upper band is 101 MHz (5420–5521 MHz). Figures 3(a)–3(d) describe the surface current distribution at the four different resonant frequencies to get a deep understanding of the operating modes. It is noted from Figure 3(a) that a strong current is concentrated at the longer strip at 900 MHz. The total current length is approximately equal to one quarter wavelength. At 3.5 GHz, from Figure 3(b), a strong concentration of surface current is seen on the upper strip, whereas at 4.2 GHz, Figure 3(c), the surface current is distributed on the periphery of the CSRR. Being the dual counterpart of conventional SRR, by the virtue of Babinet's principle and complementarity, the CSRR requires the excitation of a time varying electric field having a strong component parallel to its axis, so that it can resonate at some frequencies [21, 22]. The resulting structure behaves as a narrow band-pass structure that supports backward wave propagation [23]. At 5.5 GHz, Figure 3(d), strong concentration of surface current is distributed on the lower part of longer strip. A conclusion can be drawn from all the plots from Figures 3(a)–3(d) that each of the four resonances has resulted due to the four different parts of the proposed quad band IFA structure. Each of them behaves as a quarter wavelength resonator at their respective resonance frequencies in free space, and each of the frequency bands is independently tunable.

2.2. Independent Frequency Tuning

To note the mutual exclusiveness of each frequency band, parametric studies are carried out. For independent control, the current path responsible for each band should be identified. From the surface current distribution, Subsection 2.1, Figures 3(a)–3(d), the current path responsible for each band is identified, so that by changing the length of each current path, each frequency band can be changed. Parametric studies are carried out by varying the length and coupling of each resonator and finally see the effects of these parameters on resonant frequency and impedance matching. Figure 4 shows that W_8 can be used to vary the lower band over a wide range without affecting others. Figure 5 shows L_6 can

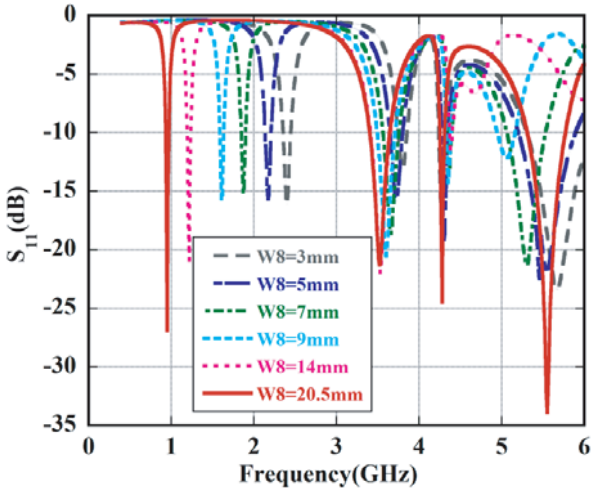

Figure 4. Effect of different values of W_8 on S_{11}.

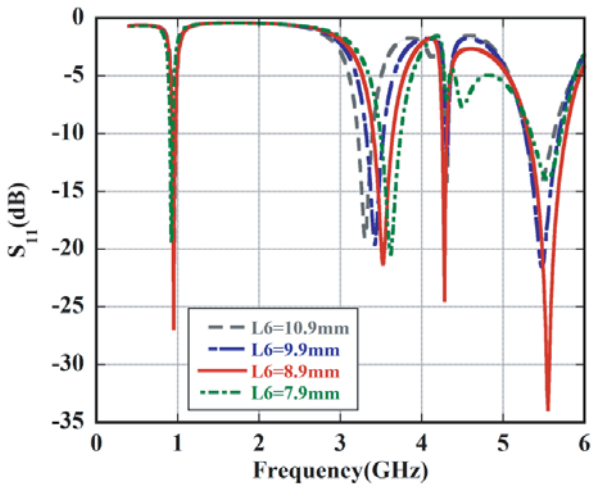

Figure 5. Effect of different values of L_6 on S_{11}.

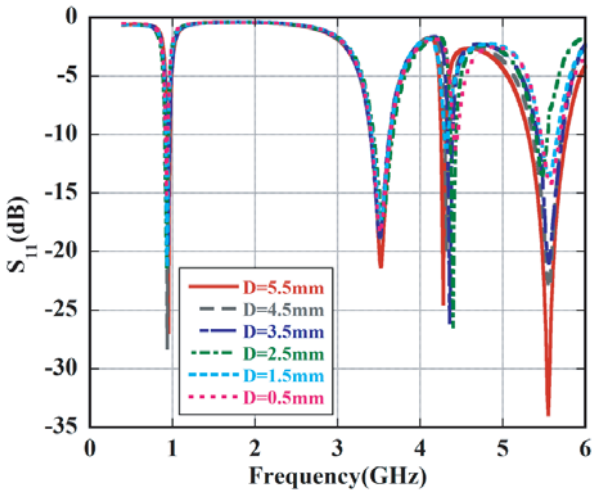

Figure 6. Effect of varying the distance D on S_{11}.

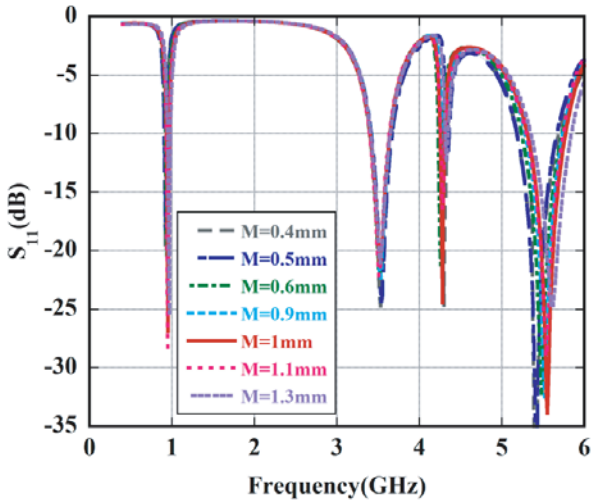

Figure 7. Effect of varying the distance M on S_{11}.

be used to vary the second band independently. Figure 6 and Figure 7 show that by varying distances M and D, the third and fourth bands are varied independently.

2.2.1. Effect of Length W_8

When length W8 is varied, a significant variation from 2.4 GHz (Wi-fi) to 0.9 GHz (GSM) covering 1.575 GHz (GPS) is attained keeping all other bands unchanged as shown in Figure 4. The lower band can be controlled over 90.9% from (0.9 GHz–2.4 GHz), since this band can be controlled over a huge bandwidth independently, this antenna can be used for different applications. The optimal length of $W_8 = 20.5$ mm ($W_8 = 14$ mm $+ L_1 = 6.5$ mm) is chosen for achieving the 0.9 GHz (GSM) band.

2.2.2. Effect of Length L_6

The second resonance is tuned by varying length L_6 as shown in Figure 5. The surface current distribution in Figure 3(b) also shows a huge concentration of current on the upper strip. The optimal length of $L_6 = 8.9$ mm is chosen for 3.5 GHz band.

2.2.3. Effect of Distances D and M

The third and fourth frequencies are tuned by varying distances D and M. The change of position of the shorting pin disturbs the current variation which in turn influences the input impedances and disturbs

Table 1. Independent control range in four bands.

Frequency Band	900 MHz	3.5 GHz	4.2 GHz	5.5 GHz
Control range (MHz)	900–2400	3276–3756	4271–4451	5405–5612
Control range (%)	90.90	13.65	4.12	3.75

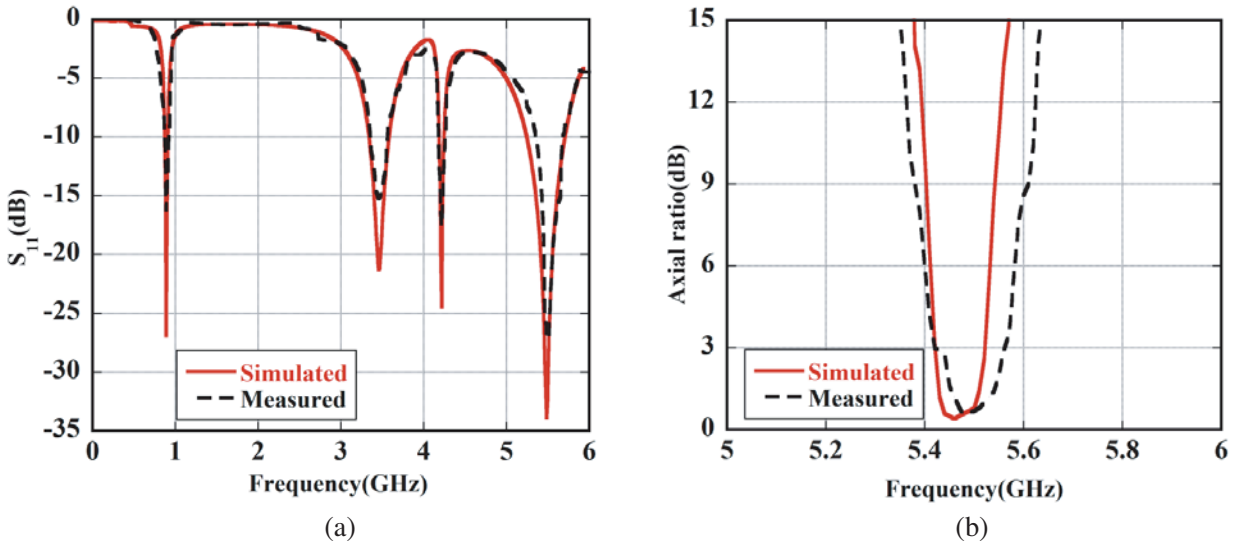

Figure 8. Simulated and measured characteristics (a) S_{11} and (b) AR.

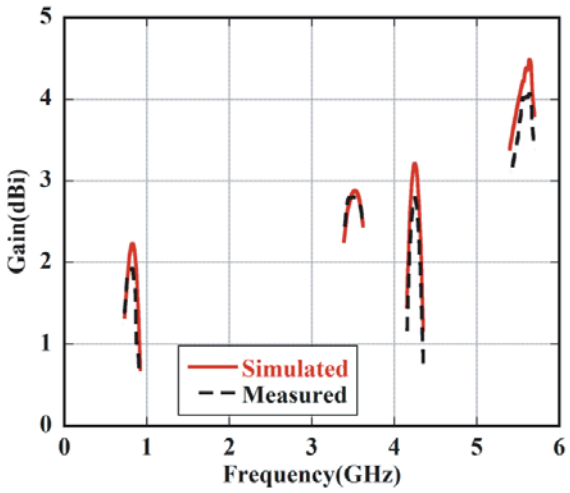

Figure 9. Simulated versus measured gain.

the current flow to the antenna. The coupling between the CSRR and IFA comes from the capacitive coupling due to the ring slot and magnetic coupling due to split of the outer ring, and consequently, this varies the third and fourth resonances as shown in Figure 6 and Figure 7, respectively. $D = 5.5\,\text{mm}$ and $M = 1\,\text{mm}$ are the optimal values for 4.2 GHz and 5.5 GHz, respectively.

3. EXPERIMENTAL RESULTS AND DISCUSSION

In this section, the proposed antenna is studied with simulated, measured, and tuning results. The reflection coefficient characteristics of simulated versus measured and the axial ratio at higher resonating frequency of the proposed antenna are presented respectively in Figures 8(a) and 8(b). There is a good

Table 2. Comparisons of antenna size and operational bandwidth among proposed antenna and other studies.

Reference No.	Antenna size (mm × mm)	Ground plane size (mm × mm)	Operational bandwidth (GHz)
3.	30 × 40	14.6 × 40	0.912–0.972 2.390–3.943 4.689–5.324
4.	43 × 8	35 × 8	2.355–5 5.112-7 (−6 dB reference)
5.	29 × 36	29 × 11	2.32–2.65 3.21–3.34 5.01–6.1
6.	24 × 30	24 × 5	2.50–2.71 3.37–3.63 5.20–5.85
7.	50 × 40	15 × 40	2.39–2.59 3.1–3.57 5.45–6.5
9.	33 × 20	33 × 13	2.25–3.5 4.5–5.25
10.	100 × 45	93 × 45	2.4–2.49 3.28–3.57 5.11–5.55
11.	50 × 12	50 × 100	0.880–0.960 1.7–2.7 4.820–6.090 (−6 dB reference)
12.	96 × 11.2	240 × 210	0.663–0.993 1.689–2.190 2.449–2.783
Proposed Antenna	**20 × 18**	**20 × 8**	**0.878–0.964** **3.393–3.655** **4.224–4.321** **5.3–5.814**

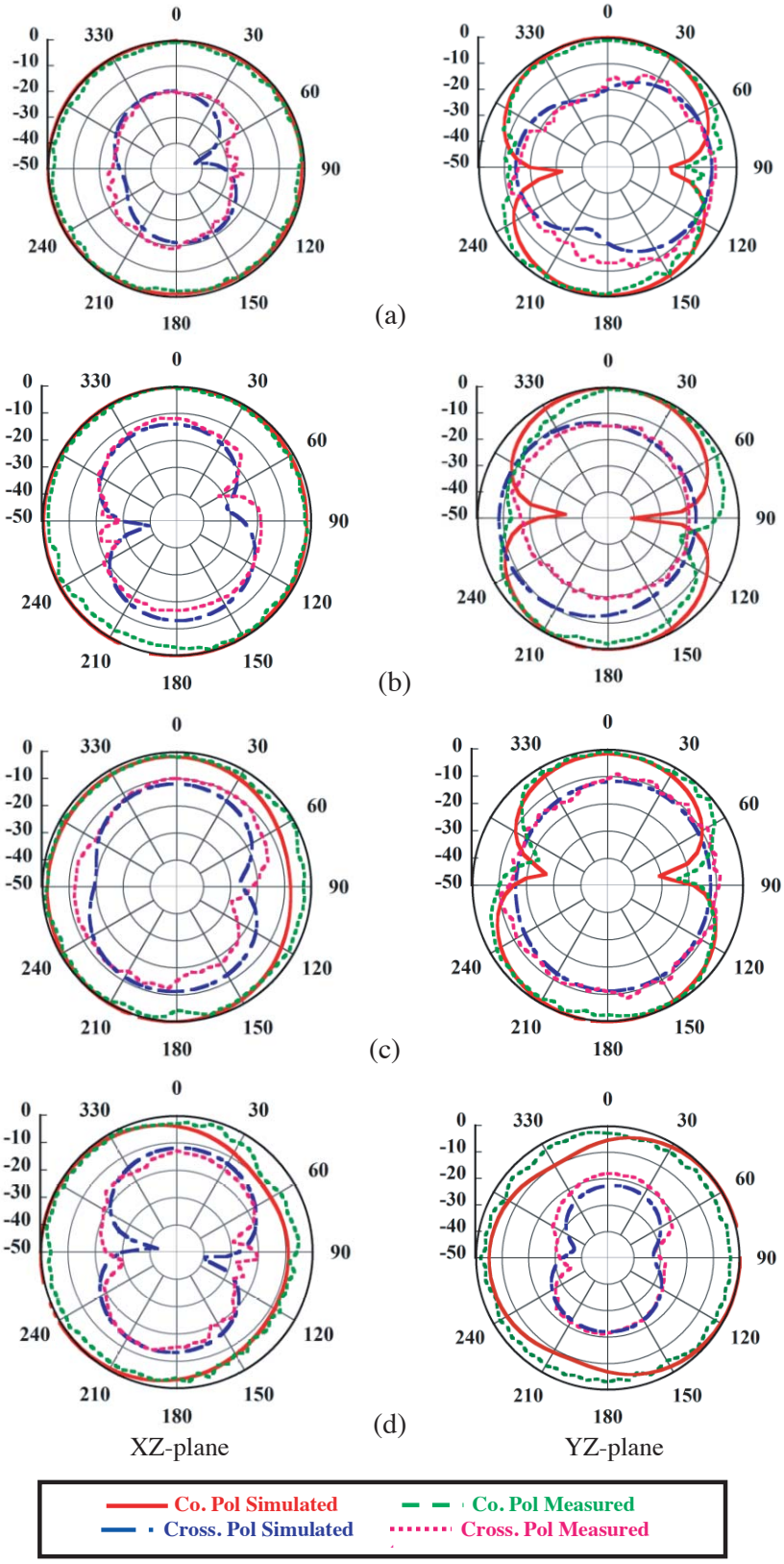

Figure 10. Simulated and measured normalized radiation patterns of proposed antenna at; (a) 0.9 GHz; (b) 3.5 GHz; (c) 4.2 GHz; (d) 5.5 GHz.

matching of reflection coefficient between the measured and simulated results for the proposed antenna shown in Figure 8(a). A CP is obtained for the fourth band with a minimum AR value of 0.41 dB at CP centre frequency f_c of 5.46 GHz having ARBW of 1.82% as shown in Figure 8(b). The gain of the proposed antenna is 2.2 dBi at 0.9 GHz, 2.8 dBi at 3.5 GHz, 3.2 dBi at 4.2 GHz, and 4.4 dBi at 5.5 GHz, respectively, as shown in Figure 9. The simulated and measured normalized co-pole and cross-pole radiation patterns are shown in Figure 10, at 0.9 GHz, 3.5 GHz, 4.2 GHz, and 5.5 GHz, respectively. Table 1 shows the control range for the other three bands which are also tuned independently. The proposed structure shows four operating frequencies (0.9 GHz/3.5 GHz/4.2 GHz/5.5 GHz) which can be used for various cellular and wireless applications. The design steps of the proposed antenna are shown in Figure 2(a). The resonant paths, longer and shorter, control the lowest (0.9 GHz) and the second band (3.5 GHz) which is again confirmed mathematically by Equation (3) and Equation (7) and also by the current distribution as in Figure 3(a) and Figure 3(b). Parametric studies shown in Figure 4 and Figure 5 show that by varying W_8 and L_6, the two bands can be tuned independently. Table 1 confirms a 90.9% of control range for the lowest band. The position of CSRR is offset to introduce the third band (4.2 GHz). The surface current distribution confirms it, Figure 3(c). The parametric studies show that by varying distance M, the 4.2 GHz band can be tuned independently. The initial IFA 1 structure introduced the 5.8 GHz and 6.4 GHz band, which at the final IFA 5 structure shifts the higher frequency to 5.5 GHz as shown in Figure 2(b). The surface current distribution and parametric studies show that the variation of D tunes the 5.5 GHz frequency band independently. In Table 2, a comparison of the proposed structure with some other antennas as reported in the references is given. It shows that the proposed antenna is very compact and thus can be used for various small form factor devices.

4. CONCLUSION

A new approach of a branch-line printed IFA structure loaded with CSRR is proposed with dual polarisations for quad band operation. The four operating frequencies are 900 MHz/3.5 GHz/4.2 GHz/5.5 GHz. The proposed structure is compact with a dimension of $20 \times 18 \times 0.8\,\text{mm}^3$. It uses two different resonant paths, with the longer one controlling the lowest resonance at 900 MHz and also 5.5 GHz, and the shorter one controlling the resonance at 3.5 GHz. The position of CSRR is offset to introduce the third resonance at 4.2 GHz. Each of the frequency bands is independently tunable with the lowest band 900 MHz having the control range of 90.90%. The gain of the proposed antenna is 2.2 dBi at 0.9 GHz, 2.8 dBi at 3.5 GHz, 3.2 dBi at 4.2 GHz, and 4.4 dBi at 5.5 GHz, respectively. The structure shows linear polarisation for the first three bands and circular polarisation for the WLAN band with ARBW of 1.82%. Thus the antenna structure is suitable for small form factor devices for quad-band applications.

REFERENCES

1. Wong, K. L., G. Y. Lee, and T. W. Chiou, "A low-profile planar monopole antenna for multiband operation of mobile handsets," *IEEE Trans. Antennas Propag.*, Vol. 51, No. 1, 353–355, 2003.
2. Wong, K. L., L. C. Chou, and C. M. Su, "Dual-band flat-plate antenna with a shorted parasitic element for laptop application," *IEEE Trans. Antennas Propag.*, Vol. 53, No. 1, 539–544, 2005.
3. Abutarboush, H. F., H. Nasif, R. Nilavalan, and S. W. Cheung, "Multiband and wide monopole antenna for GSM 900 and other wireless applications," *IEEE Antennas Wirel. Propag. Lett.*, Vol. 11, 539–542, 2012.
4. Chung, M. A. and W. H. Chang, "Low-cost, low-profile and miniaturized single-plane antenna design for an Internet of Thing device applications operating in 5G, 4G, V2X, DSRC, WiFi 6 band, WLAN, and WiMAX communication systems," *Microw Opt Technol Lett.*, 1–9, 2019, https://doi.org/10.1002/mop.32229.
5. Chandan, "Truncated ground plane multiband monopole antenna for WLAN and WiMAX applications," *IETE Journal of Research*, 1–6, 2020, DOI: 10.1080/03772063.2019.1709568.
6. Kumar, A., D. Jhanwar, and M. M. Sharma, "A compact printed multistubs loaded resonator rectangular monopole antenna design for multiband wireless systems," *Int. J. RF Microw. Comput. Aided Eng.*, Vol. 27, No. 9, 1–10, 2017.

7. Kim, D. O., C. Y. Kim, D. G. Yang, and M. S. Ahmad, "Multiband omnidirectional planar monopole antenna with two split ring resonator pairs," *Microw. Opt. Technol. Lett.*, Vol. 59, 753–758, 2017.
8. Kuo, Y. L., T. W. Chiou, and K. L. Wong, "A novel dual-band printed inverted-F antenna," *Microw. Opt. Technol. Lett.*, Vol. 31, No. 5, 353–355, 2001.
9. Khaldi, M. A., "A highly compact multiband antenna for Bluetooth/WLAN, Wi-MAX, And Wi-Fi applications," *Microw. Opt. Technol. Lett.*, Vol. 59, No. 1, 77–80, 2017.
10. Pazin, L., N. Telzhensky, Y. Leviatan, "Multiband flat-plate inverted-F antenna for Wi-Fi/WiMAX operation," *IEEE Antennas Wirel. Propag. Lett.*, Vol. 7, 197–200, 2008.
11. Chiu, C. W. and Y. J. Chi, "Planar hexa-band inverted-F antenna for portable device applications," *IEEE Antennas Wirel. Propag. Lett.*, Vol. 8, 1099–1102, 2009.
12. Hu, C. L., D. L. Huang, H. L. Kuo, C. F. Yang, C. L. Liao, and S. T. Lin, "Compact multibranch inverted-F antenna to be embedded in a laptop computer for LTE/WWAN/IMT-E applications," *IEEE Antennas Wirel. Propag. Lett.*, Vol. 9, 838–841, 2010.
13. Midya, M., S. Bhattacharjee, G. K. Das, and M. Mitra, "Dual-band dual-polarized compact planar monopole antenna for wide axial ratio bandwidth application," *Int. J. RF Microw. Comput. Aided Eng.*, 2020, https://doi.org/10.1002/mmce.22152.
14. Row, J. S. and K. W. Lin, "Low-profile design of dual-frequency and dual-polarised triangular microstrip antennas," *Electron Lett.*, Vol. 40, 156–157, 2004.
15. Kumar, P., S. Dwari, and R. K. Saini, "Triple band dual polarized CPW-fed planar monopole antenna," *Wireless Personal Commun.*, Vol. 99, 431–440, 2018.
16. Wang, Y., X. Li, L. Yang, S. X. Gong, X. Y. Feng, and J. X. Wang, "Compact triple-band dual-polarized microstrip patch antenna for wireless applications," *Microwave Opt. Technol. Lett.*, Vol. 56, 778–783, 2014.
17. Saxena, S., B. K. Kanaujia, S. Dwari, S. Kumar, and R. Tiwari, "A compact microstrip fed dual polarised multiband antenna for IEEE 802.11 a/b/g/n/ac/ax applications," *AEU-Int. J. Electron Commun.*, Vol. 72, 95–103, 2017.
18. Midya, M., S. Bhattacharjee, and M. Mitra, "Compact cpw-fed circularly polarized antenna for WLAN application," *Progress In Electromagnetics Research M*, Vol. 67, 65–73, 2018.
19. Casula, G. A., P. Maxia, G. Mazzarella, and G. Montisci, "Design of a printed log-periodic dipole array for ultra-wideband applications," *Progress In Electromagnetics Research C*, Vol. 38, 15–26, 2013.
20. Kuo, Y. L. and K. L. Wong, "Coplanar waveguide-fed folded inverted-F antenna for UMTS applications," *Microw. Opt. Technol. Lett.*, Vol. 32, No. 5, 364–366, 2002.
21. Ozanazi, V. and V. B. Erturk, "A comparative investigation of SRR-and CSRR-based band-reject filters: Simulation, Experiments, and discussions," *Microw. Opt. Technol. Lett.*, Vol. 50, No. 2, 519–523, 2008.
22. Bonache, J., F. Martin, F. Falcone, J. D. Baena, T. Lopetegi, J. Garcia-Garcia, M. A. G. Laso, I. Gil, A. Marcotegui, R. Marques, and M. Sorolla, "Application of complementary split-ring resonators to the design of compact narrow band-pass structures in microstrip technology," *Microw. Opt. Technol. Lett.*, Vol. 46, No. 5, 508–512, 2005.
23. Bonache, J., I. Gil, J. García-García, and F. Martín, "Novel microstrip bandpass filters based on complementary split-ring resonators," *IEEE Trans. Microw. Theory Tech.*, Vol. 54, No. 1, 265–271, 2006.